

Chitosan Nanoparticles Inhibit the Growth of Human Hepatocellular Carcinoma Xenografts through an Antiangiogenic Mechanism

YINGLEI XU, ZHENGSHUN WEN and ZIRONG XU

*Key Laboratory of Molecular Animal Nutrition of Ministry of Education,
College of Animal Sciences, Zhejiang University, Hangzhou, China*

Abstract. *Chitosan nanoparticles (CNP) have demonstrated anticancer activity in vitro and in vivo by a few recent researches. However, the mechanisms involved in their potential anticancer activity remain to be elucidated. In this study, the effects of CNP on tumor growth were investigated using a model of nude mice xenografted with human hepatocellular carcinoma (HCC) (BEL-7402) cells. The results demonstrated that the treatment of these nude mice with CNP significantly inhibited tumor growth and induced tumor necrosis. Furthermore, microvessel density (MVD) determination by counting immunohistologically stained tumor microvessels suggested that CNP dose-dependent tumor suppression was correlated with the inhibition of tumor angiogenesis. Mechanistically, immunohistochemical and quantitative real-time reverse transcription-polymerase reaction assays provided evidence that CNP-mediated inhibition of tumor angiogenesis was linked to impaired levels of vascular endothelial growth factor receptor 2 (VEGFR2). Due to their low or non-toxicity, CNP and their derivatives may represent a novel class of anti-cancer drug.*

Hepatocellular carcinoma (HCC) is one of the most common and deadly malignancies in the world and this disease is usually associated with chronic liver injury and cirrhosis (1-3). The most common risk factors involved in its etiology and development are viral hepatitis and chronic alcohol abuse (3, 4). The overall survival rate of patients with HCC has not been significantly improved in the last two decades (5), and no drugs are currently available to prevent or reduce

tumor spread and/or recurrence. Traditional chemotherapy and radiotherapy are avoided in the treatment of this disease due to associated liver toxicity. The only known curative therapy for HCC is surgery (either hepatic resection or complete liver transplantation), however very few patients are candidates for surgical therapy because the tumor has metastasized to locations beyond the liver or due to the lack of transplantable organs at the time of diagnosis (6). Therefore new therapies are urgently needed.

Angiogenesis is a physiological process involving the formation of new blood vessels from pre-existing vasculature. It is now well recognized that angiogenesis is important not only in normal physiological processes, but also in various diseases, especially cancer (7, 8). Under normal physiological circumstances angiogenesis is tightly regulated by a balance between angiogenic activators and inhibitors, while pathological angiogenesis, triggered by an angiogenic switch (the net balance between pro- and anti-angiogenic molecules favors angiogenesis), is crucial for tumor growth and metastasis. Vascular endothelial growth factor (VEGF) is one of the key regulators of tumor angiogenesis (9) and its pro-angiogenic effects including stimulating endothelial cell migration, proliferation, survival, and enhancing vascular permeability are primarily mediated by its cell surface tyrosine kinase receptor VEGFR2 (10). It has been demonstrated that the levels of VEGF and VEGFR2 are frequently up-regulated in tumor tissues, and the overexpression of VEGF enhances tumor growth and metastasis and is associated with poor clinical outcomes (11, 12). Therefore, the signaling through VEGF/VEGFR2 have become promising molecular targets in cancer therapy and angiogenesis inhibitors including sorafenib, which block VEGF/VEGFR2 signaling, have been developed for clinical application (13-15).

Chitosan, a cationic polysaccharide generated commercially by partial deacetylation of chitin, is useful in a variety of applications including biomedicine (16), pharmaceuticals (17), metal chelation (18), and food additives (19). Given that the efficacy of most current cancer drugs is limited by their dose-

Correspondence to: Prof. Zirong Xu, College of Animal Sciences, Zhejiang University, Huajia-chi Campus, Hangzhou 310029, P.R. China. Tel: +8657186091820, Fax: +8657186994963, e-mail: zrxu@zju.edu.cn

Key Words: Chitosan nanoparticles, hepatocellular carcinoma, tumor growth, necrosis, angiogenesis, VEGFR2.

related toxicities, nanoparticle-mediated drug delivery system that retains or increases anti-tumor activity without additional toxic side effects is highly desirable (20). Chitosan nanoparticles (CNP), formed inexpensively by the ionotropic gelation of cationic chitosan with polyanion sodium tripolyphosphate are one of the most extensively studied nanoparticles for controlled drug delivery and have shown great efficiency as potential drug carriers (21-25). Additionally, CNP-delivered drug accumulates selectively in tumor not normal tissues because of an enhanced permeation and retention effect (EPR) (26). Surprisingly, a recent study from our laboratory has found that CNP has antitumor activities *in vitro* and *in vivo* (27, 28). In the present study, the effect of CNP on tumor growth was investigated in a xenograft model using human HCC cells.

Materials and Methods

Reagents. Chitosan nanoparticles were prepared and characterized as described previously (29). The vehicle, acetic acid (HAC)/sodium tripolyphosphate solution, was used as the control in the animal studies. CNP with a mean particle size ranging from 52 nm to 73 nm and a positive surface charge of about 50 mV, regularly formed and well distributed in HAC/sodium tripolyphosphate solution (pH 5) were used in this study (Figure 1). The monoclonal VEGF antibody and factor VIII-related antigen (F8/86) antibody were purchased from Gene Tex (Southern California, USA). Polyclonal VEGFR2 antibody was purchased from Thermo Scientific (Shanghai, China). Dako EnVision+™ Peroxidase (Dako Corp., Carpinteria, California, USA), M-MLV reverse transcriptase (Promega Corp., Madison, Wisconsin, USA) UNIQ-10 Column total RNA isolation kit (Shanghai Sangon Biotech Inc., Shanghai, China), and SYBR Premix Ex-Taq Kit (TaKaRa Biotech Inc., Dalian, China) were used as directed.

Cells and cell culture. The human HCC cell line BEL-7402 was obtained from the Cell Bank of the Chinese Academy of Science (Shanghai, China). The cells were maintained in culture as previously described (28).

In vivo tumor model. Six-week-old female athymic nude mice were obtained from the Slac Laboratory Animal Limited Company (Shanghai, China) and housed in the animal facility under specific pathogen-free conditions. All the animal experiments were conducted in accordance with a protocol approved by Zhejiang University. Two million BEL-7402 cells were suspended in 250 μ l of saline solution and injected subcutaneously into the fatty layer of the anterior forelimb using sterile technique. The animals were given free access to food and water. Tumor diameters were measured every five days using a caliper, and tumor volumes were calculated by a standard formula ($\text{width}^2 \times \text{length} / 2$). Given the limitation of our previous study (a single dose and one end-time point), to further understand the pharmacokinetics and safety parameters of CNP, we investigated the effects of CNP treatment at daily oral dose levels of 0, 60 and 90 mg/kg/day on HCC tumor growth for 21 days were investigated. Once tumor growth reached 100 mm³ in size, CNP or vehicle was given by oral administration once daily to groups of six animals. After 21 days, the mice were euthanized by CO₂ followed by cervical dislocation, and the tumors

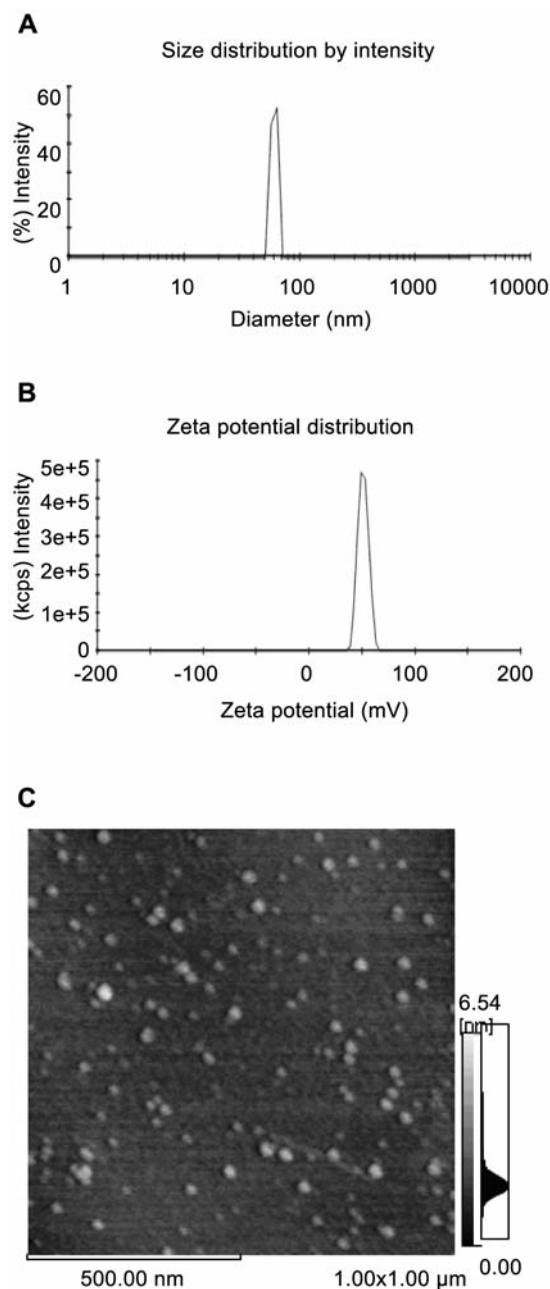


Figure 1. Size, zeta potential, and morphology of CNP. A: The size distribution by intensity of CNP. B: Zeta potential distribution of CNP. C: Atomic force micrograph (AFM) of CNP.

were excised from sacrificed animals. One-half of each tumor was immediately frozen in liquid nitrogen and then stored at -80°C until analysis. The remaining tumor halves were fixed in 10% neutral buffered formalin overnight at room temperature and then stored in 70% ethyl alcohol for subsequent histological analysis. Growth curves for the tumors in each group were plotted as a function of tumor volume (mm³; mean \pm S.D.) vs. time.

Table I. Oligonucleotide primers used for quantitative real-time RT-PCR.

Gene	Accession number	Forward primer 5'-3'	Reverse primer 5'-3'
VEGF-A	NM_001033756	CCTGGTGGACATCTTCCAGGAGTACC	GAAGCTCATCTCTCCTATGTGCTGGC
VEGFR2	AF063658	TCCCGTTAGAAGAACCAGAAGT	TGAGGCAAGAACCATACTACT
GAPDH	NM_002046	CTGCTCCTCTGTTCGACAGT	CCGTTGACTCCGACCTCAC

Accession number: The accession number of the sequence in the Entrez Nucleotide database.

Histology. The fixed tumor tissues were embedded in paraffin, sectioned at ~4 µm thicknesses and mounted onto slides. After deparaffinization and hydration, the sections were either stained with hematoxylin and eosin (H&E) or used for subsequent immunohistochemistry. The necrotic area of each tumor was quantified by morphometric determination of the proportion of the total tumor area that was necrotic in the H&E stained section.

Immunohistochemistry. The labeled polymer method was used in immunohistological staining. In brief, the sections were deparaffinized in xylene and re-hydrated in graded solutions of ethanol. Antigen retrieval was performed at 95°C for 40 min in 0.01M sodium citrate buffer (pH 6.0). All the sections were then immersed in 3% hydrogen peroxide for 30 min. After being incubated overnight with the primary antibody at 4°C, the sections were incubated with Dako EnVision+™ peroxidase for 60 min. The peroxidase reaction was visualized with "liquid 3", 3-diaminobenzidine tetrahydrochloride (DAB) and counterstained in hematoxylin. The slides were then viewed under a brightfield microscope. Positive staining was counted in a ×400 field and five randomly chosen fields per section were selected to determine the average count of microvessel density (MVD) (30). Any single highlighted endothelial cell, an endothelial cell cluster clearly separated from adjacent microvessels, or distinct clusters of brown-staining endothelial cells was counted as a separate count. The evaluation of the expression levels of VEGF and VEGFR2 was performed in accordance with the immunoreactive score (IRS) (31): IRS=SI (staining intensity) ×PP (percentage of positive cells). SI was determined as 0, negative; 1, weak; 2, moderate and 3, strong. PP was defined as 0, negative; 1, 10% positive cells; 2, 11-50% positive cells; 3, 51-80% positive cells and 4, more than 80% positive cells.

RNA isolation and reverse transcription. The total RNA was extracted from each tumor sample using an UNIQ-10 Column total RNA isolation kit according to the manufacturer's directions. The integrity and quality of each total RNA sample was analyzed by measurement of the optical density at 260/280 nm and verified by inspection of the 18S and 28S rRNA bands after agarose gel electrophoresis. The total RNA (2 µg) was reversely transcribed using M-MLV reverse transcriptase according to the manufacturer's protocol.

Real-time quantitative RT-PCR. Real-time quantitative PCR was used to quantify the mRNA expression of total glyceraldehyde-3-phosphate dehydrogenase (GAPDH), VEGF and VEGFR2. Primers (Table I) were designed for GAPDH, VEGF and VEGFR2 using Primer Express® software v2.0 from Applied Biosystems. Real-time quantitative RT-PCR was performed in a 25 µl reaction volume

containing 1 µl cDNA template, 12.5 µl SYBR Premix Ex Taq™ (2×) and 1 µl forward and reverse primers (20 nM) using an iQ™ 5 real-time multicolor PCR detection system (Bio-Rad, California, USA). The real-time PCR parameters used for examining the mRNA levels were for VEGF, initial denaturation at 95°C for 10 sec, followed by 45 cycles of 5 sec denaturation at 94°C, 30 sec annealing and extension at 63°C; for VEGFR2, initial denaturation at 95°C for 10 sec, followed by 45 cycles of denaturation at 95°C for 5 sec, annealing at 58°C for 10 sec and elongation at 72°C for 8 sec, and for GAPDH, initial denaturation at 95°C for 10 sec, followed by 45 cycles of denaturation at 95°C for 5 sec, annealing and extension at 60°C for 20 sec. The fluorescence signals for VEGF, VEGFR2 and GAPDH were collected at 63°C, 72°C and 60°C respectively. Melting curves were all made from 55°C – 95°C to determine the specificity of the amplification reactions. The relative amount of target mRNA was calculated by the 2^{-ΔΔCt} method (32), while all the gene expression values were normalized to that of GAPDH in the same sample.

Statistical analysis. The results are presented as the means±SD. ANOVA was used to determine the differences between control and treated groups. *P*<0.05 was considered significant. Analysis was performed using the SAS system for windows v6.12 (SAS Institute Inc., North Carolina, USA).

Results

Effects of CNP on xenograft growth. As shown in Figure 2 the growth of the xenografts was strongly inhibited by CNP treatment in a time- and dose-dependent pattern. In addition, all the CNP-treated mice showed no signs of neurological toxicity or weight loss and none of the mice died during this study, suggesting that oral administration of CNP is safe in this mouse model.

Effect of CNP on tumor necrosis. As shown in Figure 3. A-C, in the vehicle group the tumors were composed predominantly of tightly packed carcinoma cells. In contrast, the CNP treatment clearly induced "hollow-like" necrosis in the center, as shown by the appearance of the histological features in the regressing tumor. These histological differences were quantified by morphometric determination of the proportion of total tumor area that was necrotic in H&E staining section. As indicated in Figure 3D, the necrotic area of the tumors treated with CNP dramatically increased compared to the controls in a dose-dependent manner.

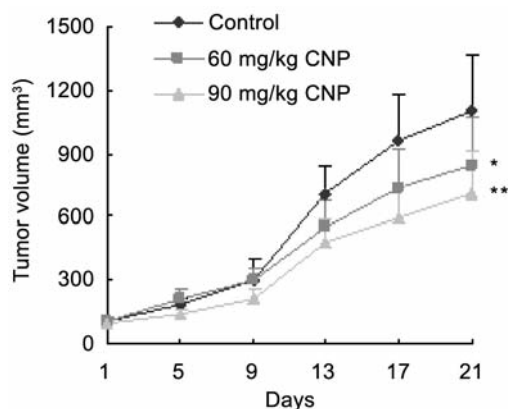


Figure 2. Effect of CNP on hepatocellular carcinoma xenografts growth. * $p < 0.05$, ** $p < 0.01$ compared with the control.

Effect of CNP on tumor angiogenesis. The angiogenesis in each tumor section was assessed by factor VIII-related antigen (F8/86) staining. As shown in Figure 4A-C, abundant capillary-like nets were found in the sections from the vehicle group (A), while only a few were observed in the sections from mice treated with CNP (B, C). The degree of angiogenesis (MVD) was quantified by counting the number of positive microvessels. As shown in Table II, compared to that of the vehicle alone group, the average number of factor VIII-related antigen (F8/86)-positive microvessels in the CNP-treated mice was reduced in a dose-dependent pattern.

Effect of CNP on VEGF and VEGFR2 gene expression. CNP had no effect on VEGF mRNA (Figure 5A) and protein expression (Figure 4D-F and Table II) compared with that of the vehicle group, while the levels of VEGFR2 mRNA (Figure 5B) and protein (Figure 4G-I and Table II) were significantly reduced by CNP treatment, suggesting that CNP inhibited angiogenesis of HCC by suppressing VEGFR2 expression.

Discussion

A new observation emerging from our recent studies (27, 28) suggested that CNP has strong antitumor activities. *In vitro*, CNP treatment of human tumor cells induced apoptosis and growth suppression. It has been suggested that CNP acts at multiple levels to induce HCC cell (BEL-7402) death, including disrupting the cell membrane, decreasing the negative surface charge and mitochondrial membrane potential, inducing lipid peroxidation, disturbing the fatty acid composition of the membrane and fragmenting DNA (33). *In vivo*, CNP also showed significant dose- and size-dependent antitumor activity against Sarcoma-180 and hepatoma H22 in mice. These findings suggested CNP itself

Table II. MVD and immunoreactive score for VEGF and VEGFR2 in xenografts.

Group	n	MVD	VEGF	VEGFR2
The Control	6	28.67±6.35	6.81±0.88	7.14±0.93
60mg/kg CNP	6	21.67±2.58*	8.14±1.1	5.13±0.87**
90mg/kg CNP	6	16.33±4.68**	7.55±0.8	4.97±0.65**

* $p < 0.05$, ** $p < 0.01$ compared with the control. MVD: microvessel density, VEGF: vascular endothelial growth factor, VEGFR2: VEGF receptor 2.

may be a novel class drug for the treatment of cancer including HCC.

The mechanism by which CNP inhibits *in vivo* tumor growth still remains elusive. Similar to many other tumors, HCC growth is partly determined by the balance between cell proliferation and apoptosis. The induction of necrotic effects in the tumor is one of the key mechanisms of most anticancer drugs (20). Therefore, a possible simple explanation for CNP-mediated growth inhibition of HCC is that CNP might directly inhibit cell proliferation and induce apoptosis in tumor cells. As mentioned earlier, our previous *in vitro* studies demonstrated that, while CNP does not kill normal cells, it markedly decreases cell viability and induces DNA fragmentation *in vitro*, suggesting that CNP has potent and specific cytotoxic effects on tumor cells. In the present study, tumor growth inhibition and necrosis were significantly induced by CNP treatment. This could have been due to a combined effect of a large increase in the number of apoptotic cells with a large decrease in the proportion of proliferating tumor cells. However, further evaluation by TUNEL (apoptosis) and/or K21 staining (cell proliferation) is necessary to determine whether the induction of tumor suppression and necrosis is due to the *in vivo* necrotic and/or cytostatic effects of CNP treatment.

Since chitosan has been shown to inhibit angiogenesis *in vitro* (34), the *in vivo* growth inhibition and necrosis induction of HCC by CNP may be assumed to relate to its potential anti-angiogenic effect. This hypothesis was supported by the MVD analysis in the present study, which revealed a significant reduction of factor VIII-related antigen (F8/86)-positive vessels in the tumor sections from the CNP-treated mice. Furthermore, real-time quantitative RT-PCR and immunohistochemical analysis demonstrated that CNP treatment significantly reduced VEGFR2 expression at both the mRNA and protein levels.

In summary, CNP treatment results in a dose- and time-dependent growth inhibition of human hepatocellular carcinoma in a mouse xenograft model. The antitumor activity of CNP appears to be related to its antiangiogenic activity, which is correlated with VEGFR2 production and subsequent blockage of VEGF-induced endothelial cell activation.

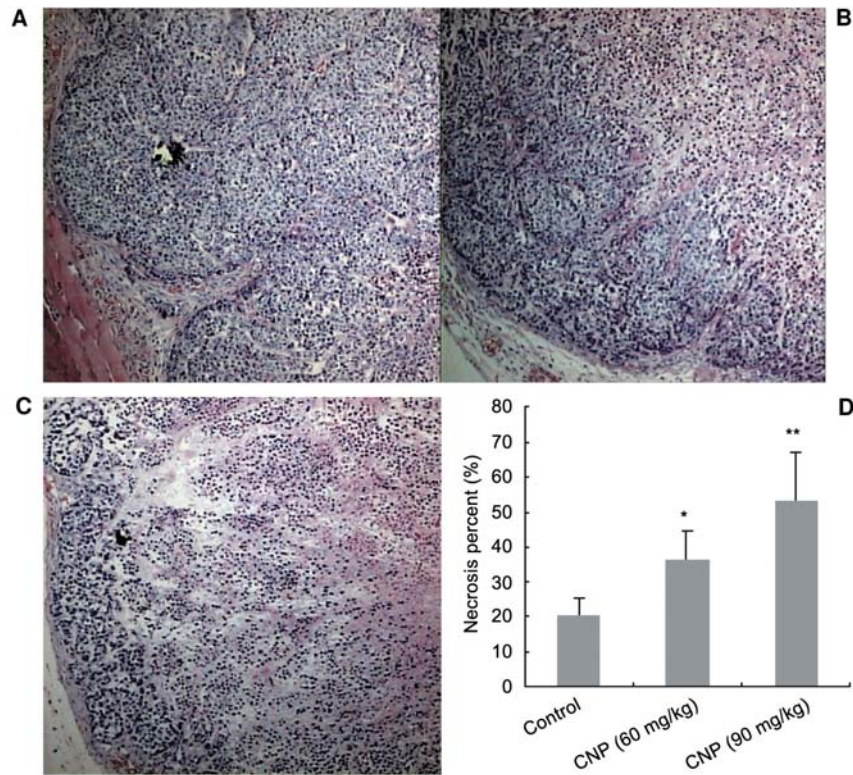


Figure 3. H&E staining of tumor sections ($\times 100$). A Control, B 60 mg/kg CNP, C 90 mg/kg CNP treated tumors. D Quantification of necrosis percentage in tumor area. * $p < 0.05$, ** $p < 0.01$ compared with the control.

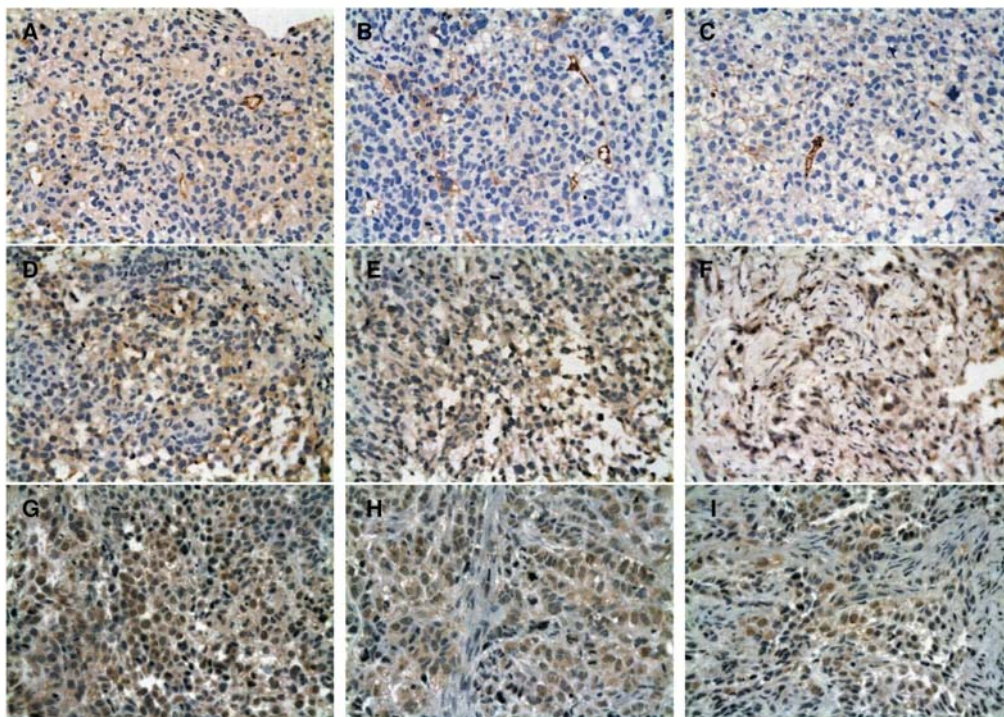


Figure 4. Immunohistochemical staining of tumor sections using Factor VIII-related antigen antibody (A-C), monoclonal VEGF antibody (D-E) and polyclonal VEGFR2 antibody (G-I) ($\times 400$). Control (A, D, G); 60 mg/kg CNP (B, E, H); 90 mg/kg CNP (C, F, I).

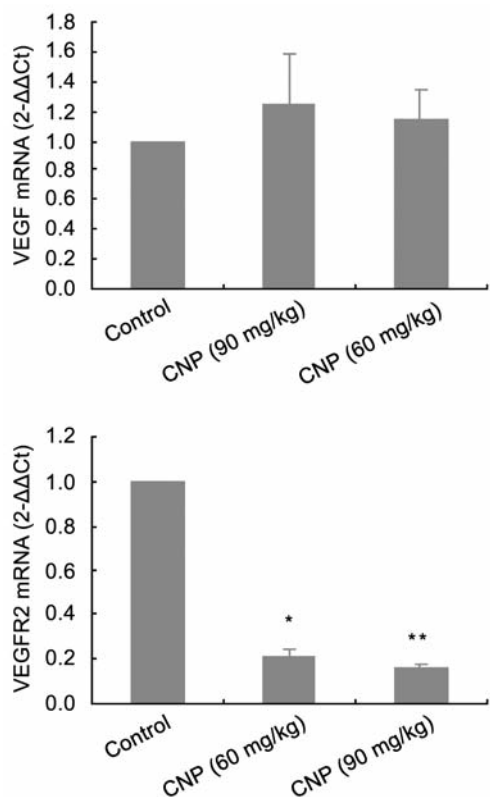


Figure 5. Effects of CNP on transcription of VEGF and VEGFR2. * $p < 0.05$, ** $p < 0.01$ compared with the control.

Acknowledgements

We thank the Centre of Laboratory Animal Research, Zhejiang College of Traditional Chinese Medicine for providing the place and conditions to raise the nude mice. This work was financially supported by Ningbo Puai Biotech, Co., Ltd.

References

- 1 Kew MC: Epidemiology of hepatocellular carcinoma. *Toxicology 181-182*: 35-38, 2002.
- 2 Okuda K: Hepatocellular carcinoma – history, current status and perspectives. *Dig Liver Dis 34*: 613-616, 2002.
- 3 Bergsland EK and Venook AP: Hepatocellular carcinoma. *Curr Opin Oncol 12*: 357-361, 2000.
- 4 La Vecchia C: Alcohol and liver cancer. *Eur J Cancer Prev 16*: 495-497, 2007.
- 5 Forner A, Hessheimer AJ, Isabel RM and Bruix J: Treatment of hepatocellular carcinoma. *Critl Rev Oncol/Hematol 60*: 89-98, 2006
- 6 Befeler AS and Di Bisceglie AM: Hepatocellular carcinoma: diagnosis and treatment. *Gastroenterol 122*: 1609-1619, 2002.
- 7 Carmeliet P and Jain RK: Angiogenesis in cancer and other diseases. *Nature 407*: 249-257, 2000.

- 8 Pralhad T, Madhusudan S and Rajendrakumar K: Concept, mechanisms and therapeutics of angiogenesis in cancer and other diseases. *J Pharm Pharmacol 55*: 1045-1053, 2003.
- 9 Roskoski R Jr: Vascular endothelial growth factor (VEGF) signaling in tumor progression. *Critl Rev Oncol/Hematol 62*: 179-213, 2007.
- 10 Shibuya M and Claesson-Welsh L: Signal transduction by VEGF receptors in regulation of angiogenesis and lymphangiogenesis. *Exp Cell Res 312*: 549-560, 2006.
- 11 Shweiki D, Itin A, Soffer D and Keshet E: Vascular endothelial growth factor induced by hypoxia may mediate hypoxia-initiated angiogenesis. *Nature 359*: 843-845, 1992.
- 12 Zhang HT, Craft P, Scott PA, Marina Z, Weich HA, Harris AL and Bicknell R: Enhancement of tumor growth and vascular density by transfection of vascular endothelial cell growth factor into MCF-7 human breast carcinoma cells. *J Natl Cancer Inst 87*: 213-219, 1995.
- 13 Witte L, Hicklin DJ, Zhu Z, Pytowski B, Kotanides H, Rockwell P and Bohlen P: Monoclonal antibodies targeting the VEGF receptor-2 (Flk1/KDR) as an anti-angiogenic therapeutic strategy. *Cancer Metast Rev 17*: 155-161, 1998.
- 14 Abou-Alfa GK, Schwartz L, Ricci S, Amadori D, Santoro A, Figuer A, Greve JD, Jean-Yves D, Lathia C, Schwartz B, Taylor I, Moscovici M and Leonard BS: Phase II study of sorafenib in patients with advanced hepatocellular carcinoma. *J Clin Oncol 24*: 4293-4300, 2006.
- 15 Wilhelm SM, Adnane L, Newell P, Villanueva A, Llovet JM and Lynch M: Preclinical overview of sorafenib, a multikinase inhibitor that targets both Raf and VEGF and PDGF receptor tyrosine kinase signaling. *Mol Cancer Ther 7*: 3129-3140, 2008.
- 16 Berger J, Reist M, Chenite A, Felt-Baeyens O, Mayer JM and Gurny R: Pseudo-thermosetting chitosan hydrogels for biomedical application. *Int J Pharm 288*: 17-25, 2005.
- 17 Valérie D, and Vinod DV: Pharmaceutical applications of chitosan. *Pharm Sci Tech Today 1*: 246-253, 1998.
- 18 Sugunan A, Thanachayanont C, Dutta J and Hilborn JG: Heavy-metal ion sensors using chitosan-capped gold nanoparticles. *Sci Tech of Adv Mater 6*: 335-340, 2005.
- 19 Shahidi F, Arachchi JKV and Jeon YJ: Food applications of chitin and chitosans. *Trends Food Sci Tech 10*: 37-51, 1999.
- 20 Mailloux A, Grenet K, Bruneel A, Bénéteau B, Vaubourdolle M and Baudin B: Anticancer drugs induce necrosis of human endothelial cells involving both necrosis and apoptosis. *Eur J Cell Biol 80*: 442-849, 2001.
- 21 Janes KA, Calvo P and Alonso MJ: Polysaccharide colloidal particles as delivery systems for macromolecules. *Adv Drug Deliver Rev 47*: 83-97, 2001.
- 22 Illum L: Chitosan and its use as a pharmaceutical excipient. *Pharmacol Res 15*: 1326-1331, 1998.
- 23 Agnihotri SA, Mallikarjuna NN and Aminabhavi TM: Recent advances on chitosan-based micro- and nanoparticles in drug delivery. *J Controlled Release 100*: 5-28, 2004.
- 24 De Campos AM, Diebold Y, Carvalho EL, Sanchez A and Alonso MJ: Chitosan nanoparticles as new ocular drug delivery systems: *in vitro* stability, *in vivo* fate, and cellular toxicity. *Pharmacol Res 21*: 803-810, 2004.
- 25 Krauland AH and Alonso MJ: Chitosan/cyclodextrin nanoparticles as macromolecular drug delivery system. *Int J Pharm 340*: 134-142, 2007.

- 26 Brannon-Peppas L and Blanchette JO: Nanoparticle and targeted systems for cancer therapy. *Adv Drug Delivery Rev* 56: 1649-1659, 2004.
- 27 Qi L and Xu Z: *In vivo* antitumor activity of chitosan nanoparticles. *Bioorgan Med Chem Lett* 16: 4243-4245, 2006.
- 28 Qi L, Xu Z, Jiang X, Li Y and Wang M: Cytotoxic activities of chitosan nanoparticles and copper-loaded nanoparticles. *Bioorgan Med Chem Lett* 15: 1397-1399, 2005.
- 29 Qi L, Xu Z, Jiang X, Hu C and Zou X: Preparation and antibacterial activity of chitosan nanoparticles. *Carbohydr Res* 339: 2693-2700, 2004.
- 30 Weidner N: Current pathologic methods for measuring intratumoral microvessel density within breast carcinoma and other solid tumors. *Breast Cancer Res Tr* 36: 169-180, 1995.
- 31 Friedrichs K, Gluba S, Editmann H and Jonat W: Overexpression of P53 and prognosis in breast cancer. *Cancer* 72: 3641-3647, 1993.
- 32 Kenneth JL and Thomas DS: Analysis of relative gene expression data using real-time quantitative PCR and the $2^{-\Delta\Delta CT}$ method. *methods* 25: 402-408, 2001.
- 33 Qi L, Xu Z and Chen M: *In vitro* and *in vivo* suppression of hepatocellular carcinoma growth by chitosan nanoparticles. *Eur J Cancer* 3: 184-193, 2007.
- 34 Harish Prashanth KV and Tharanathan RN: Depolymerized products of chitosan as potent inhibitors of tumor-induced angiogenesis. *Biochim Biophys Acta* 1722: 22-29, 2005.

Received May 14, 2009

Revised November 27, 2009

Accepted November 27, 2009